Magnetic-field-controlled quantum critical points in the triangular antiferromagnetic Cs_2 CuCl_4 − x Br_x mixed system

Natalija van Well, Sitaram Ramakrishnan, Ketty Beauvois, Navid Qureshi, E. Ressouche, Markos Skoulatos, Robert Georgii, Oksana Zaharko, Sander van Smaalen

annalen der physik
www.ann-phys.org

Magnetic-Field-Controlled Quantum Critical Points in the Triangular Antiferromagnetic $Cs_2CuCl_{4-x}Br_x$ Mixed System

Natalija van Well, Sitaram Ramakrishnan, Ketty Beauvois, Navid Qureshi, Eric Ressouche, Markos Skoulatos, Robert Georgii, Oksana Zaharko, and Sander van Smaalen*

The triangular antiferromagnetic $Cs_2CuCl_{4-x}Br_x$ mixed system is studied by neutron single-crystal diffraction in magnetic field. It shows a rich magnetic phase diagram consisting of four regimes depending on the Br concentration and is characterized by different exchange coupling mechanisms. For the investigated compositions from regime I ($0 < x \leq 1.5$), a critical magnetic field B_c is found for a Br concentration $x = 0.8$ at $B_c = 8.10(1)$ T and for $x = 1.1$ at $B_c = 7.73(1)$ T and from regime IV ($3.2 < x < 4$) for $x = 3.3$ at $B_c = 0.99(3)$ T. For magnetic fields larger than the respective B_c, magnetic superlattice reflections of these compounds are not found. The incommensurate magnetic wave vector $q = (0, 0.470, 0)$ appears below the ordering temperature $T_N = 0.51(1)$ K for $Cs_2CuCl_{3.2}Br_{0.8}$, and $q = (0, 0.418, 0)$ below $T_N = 1.00(6)$ K for $Cs_2CuCl_{0.3}Br_{3.7}$. Neutron diffraction experiments at around 60 mK for $x = 3.7$ in a magnetic field show the critical magnetic field at $B_c = 7.94(16)$ T and the formation of the second magnetic phase at around 8.5 T depending on the temperature. Inelastic neutron scattering experiments for the compound from regime III ($2 < x \leq 3.2$) with $x = 2.2$ show dynamical correlations at a temperature around 50 mK giving evidence for a spin liquid phase.

1. Introduction

One of the most important groups of the family of low-D quantum-frustrated magnets is represented by a spin-1/2 triangular lattice antiferromagnet.[1–4] The mixed compounds of $Cs_2CuCl_{4-x}Br_x$ are model anisotropic triangular lattice materials, where Cu^{2+} ions with spin-1/2 form chains (J) that are coupled in zig-zag manner (J') to form 2D frustrated planes in the bc-plane. Neighboring layers are coupled by an exchange (J'') in the a-direction (see **Figure 1**).

The different magnetic properties in the magnetic field, for example, the critical magnetic field values (B_c) of the end members along the a-axis with 8.44 and 30.71 T, respectively, for Cs_2CuCl_4 and Cs_2CuBr_4, demonstrate a big difference.[5,6] In addition, in the case of Cs_2CuBr_4, also relatively big difference between the suggested value for ratio $J'/J = 0.74$ by Ono et al., and the result published by Zvyagin et al. with $J'/J = 0.41$, measured in high magnetic field, is stated.[6,7] Apart from that, for Cs_2CuCl_4 the ratio $J'/J = 0.37$ by Ono et al., and the result published by Zvyagin et al. of $J'/J = 0.30$, measured in high magnetic field, are in good agreement with the estimated $J'/J = 0.34$ from neutron scattering experiments.[6–8]

Prof. N. van Well
Department of Earth and Environmental Sciences
Crystallography Section
Ludwig-Maximilians-University Munich
Munich D-80333, Germany
E-mail: natalija.van-well@lrz.uni-muenchen.de

Prof. N. van Well, S. Ramakrishnan, Prof. S. van Smaalen
Laboratory of Crystallography
University of Bayreuth
Bayreuth 95447 Germany

Prof. N. van Well, Dr. O. Zaharko
Laboratory for Neutron Scattering and Imaging
Paul Scherrer Institute
Villigen CH-5232 Switzerland

Dr. K. Beauvois, Dr. N. Qureshi
Science Division Diffraction Group
Institute Laue Langevin
Grenoble F-38042 France

Dr. E. Ressouche
Université Grenoble Alpes, CEA, IRIG, MEM, MDN
Grenoble F-38000 France

Dr. M. Skoulatos, Dr. R. Georgii
Heinz Maier-Leibnitz Zentrum (MLZ)
Technische Universität München
Lichtenbergstr. 1 Garching 85747, Germany

Dr. M. Skoulatos, Dr. R. Georgii
Physik Department E21
Technische Universität München
James-Franck-Str. Garching 85747, Germany

The ORCID identification number(s) for the author(s) of this article can be found under https://doi.org/10.1002/andp.202000147

DOI: 10.1002/andp.202000147

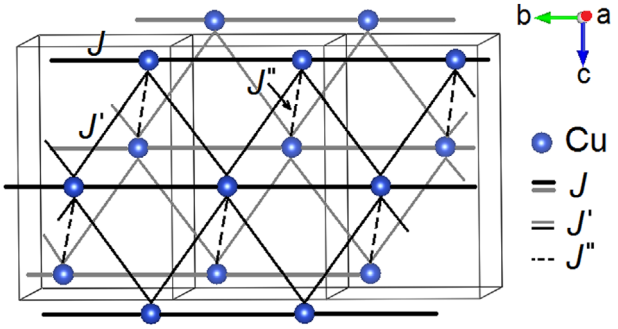

Figure 1. Magnetic exchange interaction scheme between Cu^{2+} ions within the *bc*-plane for Cs_2CuCl_4.

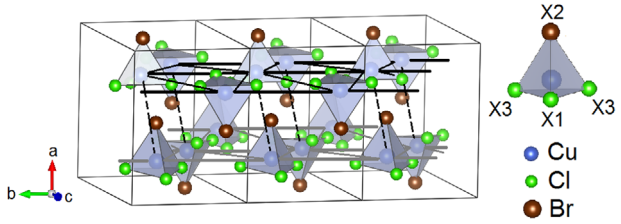

Figure 2. Left: crystal structure for $x = 1$ with the [CuCl3Br1] tetrahedra for three neighboring unit cells in the *ab*-plane. Right: [CuX4] tetrahedra with Cl and Br having different preferred occupation of the different X_i crystallographic sites. For a Br concentration with $x = 1$, the crystallographic position X2 is fully occupied by Br. Cs atoms are not shown for clarity.

The end members Cs_2CuCl_4 and Cs_2CuBr_4 show antiferromagnetic ordering at temperatures of $T_N = 0.62$ K and $T_N = 1.4$ K, respectively, in zero-field.[5,6] By applying the critical magnetic field $B_C = 8.44$ T along the *a*-direction, a quantum phase transition for Cs_2CuCl_4 into a fully polarized ferromagnetic state could be induced.[8–11] In the case of Cs_2CuBr_4, the magnetic ordering can be supressed by magnetic field along the *a*-direction at 30.71 T.[6,12]

Neutron diffraction measurements of Cs_2CuCl_4 have shown different magnetic behaviors depending on the direction of the applied magnetic field. In contrast to the magnetic fields applied along the *a*-axis, for fields along the *c*-axis, no incommensurate magnetic superlattice reflections are found for magnetic fields larger than 1.66 T, though from bulk measurements, the saturation field is 8.0 T.[8–11,13] The magnetic excitations in Cs_2CuCl_4, which have been measured using inelastic neutron scattering, show an asymmetric dispersion relation due to the competing interchain exchange interactions, which have produced an incommensurate order in the ground state.

The magnetic structure for Cs_2CuCl_4 is incommensurate along the chain direction with a temperature-independent ordering wave vector $q = (0, 0.472, 0)$.[5] The magnetic structure is cycloidal in zero magnetic field with spins rotating in the *bc*-plane. According to the prediction of the mean field theory, in an applied magnetic field, a cone structure is formed as a result of the competition between the applied field and the exchange interactions.[8,9]

Neutron diffraction measurements of Cs_2CuBr_4 of the ordering vector $q = (0, 0.575, 0)$ in the magnetic field up to 14.5 T along the *a*-axis show an anomaly at a critical field around 7.5 T. This was also observed in specific heat as a cusp-like anomaly and in the field derivative of magnetization as a small hump.[6,13] The *q* value increases with a rising magnetic field along the *c*-axis up to the magnetization plateau between 13.1 and 14.4 T. The *q* value in this plateau remains constant.[6]

For Cs_2CuBr_4, an incommensurate structure occurs below $T_N = 1.4$ K with an ordering vector $q = (0, 0.575, 0)$.[6] The magnetic structure was described as a helical structure also with spins rotating in the *bc*-plane.[6]

Therefore, it is necessary to investigate the compositions of the mixed system $Cs_2CuCl_{4-x}Br_x$ in a magnetic field to track the differences of their magnetic behavior. The experiments on the solid solution $Cs_2CuCl_{4-x}Br_x$ with a Br concentration range from 0 to 4 revealed a pronounced difference in the Cu coordination due to the increasing Br.[14] In the whole concentration range, the compounds are isostructural with space group *Pnma*.[14] At low temperatures, the crystal structures remain orthorhombic without any structural phase transition down to 50 mK, evidenced by previous neutron diffraction experiments.[15] Particularly, the anisotropy of the thermal expansion varies for different Br concentrations, leading to distinct changes of the local geometry of the $[Cu^{2+}]$ environment as a function of the respective composition.[16] Structure investigations with X-ray powder diffraction show a preferential occupation of certain sites by either Cl or Br in the [CuX4] tetrahedra, which leads to a selective occupation.[14] **Figure 2** shows the crystal structure for a Br concentration with $x = 1$.

The position of the incommensurate magnetic reflection *k* and the T_N depending on the Br concentration was recently investigated according to van Well et al.[15] The compositions of the mixed system $Cs_2CuCl_{4-x}Br_x$ of regimes I and IV also show the incommensurate structure with the ordering vector *q*, which is *x* dependent.[15]

In this study, we compare the results of neutron diffraction in magnetic field along the *a*-direction for all investigated compositions with the already published ones for the end members Cs_2CuCl_4 and Cs_2CuBr_4. Only the strongest reflections with the position (0, *k*, 0) will be presented, while the intensity of other measured reflections is much weaker. Further experiments are needed to collect datasets of sufficient quality. For investigated novel compositions, the relation between the *k*-value for the (0, *k*, 0) magnetic reflection and the wave vector *q* is $q = (0, 1-k, 0)$, same as for Cs_2CuCl_4 with the position of the incommensurate magnetic reflection $k = 0.528$ and $q = (0, 0.472, 0)$.[5] For Cs_2CuBr_4, only one reflection was examined, whose position was the same as that of the incommensurate magnetic wave vector $q = (0, 0.575, 0)$.[6]

2. Results and Discussions

Neutron diffraction experiments in magnetic field were performed for compositions with $x = 0.8$, 1.1, 3.3, and 3.7. All these compounds show magnetic ordering at zero-field. Scans through the (0 *k* 0) magnetic reflections with increasing temperature demonstrate that the intensity of the magnetic reflection decreases, when the temperature approaches the Néel point T_N. In regime I for $x = 1.1$, the Néel temperature was observed at $T_N = 0.34(1)$ K. As the phase transition temperature for $x = 0.8$ in

zero magnetic field was not measured, for the calculation of the critical magnetic field for $x = 0.8$, we have used $T_N = 0.51(1)$ K from an earlier publication, which was measured for a Br concentration of $x = 0.82$.[15] In regime III for $x = 3.3$, we have observed $T_N = 0.33(1)$ K, and for $x = 3.7$ $T_N = 1.00(6)$ K.

For the compound $Cs_2CuCl_{3.2}Br_{0.8}$, a well-defined magnetic peak was detected close to the half-integer value (0, 0.530(2), 0). Measurements in the magnetic field along the *a*-direction at temperatures of 70, 120, 180, and 300 mK were performed. **Figure 3**a) displays the intensity of (0, 0.530(2), 0) depending on selected values of the magnetic field at 70 mK. Thereafter, the magnetic satellite reflections (0, *k*, *l*) with $k = \pm 0.470$, $l = \pm 1$, and $k = \pm 1.530$, $l = \pm 1$ in the *bc*-plane were measured at a temperature of 70 mK. For *l*-even and *l*-odd, two different groups of magnetic peaks were detected. The magnetic peaks of *l*-odd are displaced symmetrically and opposite from the half-odd-integer values of *k* as compared with the peaks of *l*-even. A single peak is observed for *l*-even, for example, at the (0, ±0.530(2), ±2) positions, while for Cs_2CuCl_4 two reflections at the (0, ±0.472, ±2) and (0, ±0.528, ±2) positions were found. The position of the observed magnetic reflections notifies that the wave vector is modulated along the *b*-axis. The single ordering vector $q = (0, 0.470, 0)$ is sufficient to index all measured magnetic peaks. Thus, it is a single-*q* magnetic order incommensurately modulated along the *b*-axis.

As the incommensurate wave vector for this compound with $x = 0.8$ $q = (0, 0.470, 0)$ was determined.

Figure 3b presents the integrated intensity of *q*-scans for the magnetic reflection of $Cs_2CuCl_{3.2}Br_{0.8}$ at 70 mK as a function of the magnetic field. The results show that the 3D incommensurate magnetic order is stable up to the full ferromagnetic alignment by applying the critical magnetic field $B_c = 8.10(1)$ T. For $x = 0.8$, the *k*-value of the magnetic peak is 0.530(2), which changes smoothly with temperature. This value is stable up to 3 T and increases above 3 T (see Figure 3c). The magnetic Bragg peaks move from $k = 0.530(2)$ in zero field to $k = 0.559(5)$ at 8 T. This behavior is like the one described for Cs_2CuCl_4.[8,9]

The compositions with $x = 1.1$ and $x = 3.3$ were investigated in a magnetic field up to 9.5 T along the *a*-direction, using omega scans (rocking curves). For compound $Cs_2CuCl_{2.9}Br_{1.1}$, a magnetic peak was observed for $k = 0.516(3)$. The results reveal that no further magnetic reflections can be observed above the critical magnetic field $B_c = 7.73(1)$ T. For both compounds with $x = 0.8$ and $x = 1.1$, the critical magnetic field is smaller than that for Cs_2CuCl_4.[8,9,11] A magnetic peak for the compound $Cs_2CuCl_{0.7}Br_{3.3}$ was observed for $k = 0.560(4)$. The critical magnetic field $B_c = 0.99(3)$ T for this composition is much smaller in comparison to that of Cs_2CuCl_4 and Cs_2CuBr_4. This is due to the composition with $x = 3.3$ being close to the quantum critical point, which seems to be near $x = 3.2$.[15]

For the composition $Cs_2CuCl_{0.3}Br_{3.7}$, a magnetic peak (0, *k*, *l*) was detected for $k = 0.582(1)$. The magnetic reflections with $k = \pm 0.418$, $l = \pm 1$, and $k = \pm 1.582$, $l = \pm 1$ in the *bc*-plane were measured at a temperature of 60 mK. In analogy to the other composition, the incommensurate wave vector for $Cs_2CuCl_{0.3}Br_{3.7}$ is $q = (0, 0.418, 0)$.

The inset of **Figure 4**a presents the in tegrated intensity of *q*-scans for the magnetic reflection (0, 0.582, 0) of $Cs_2CuCl_{0.3}Br_{3.7}$ at 60 mK as a function of the magnetic field along the *a*-direction.

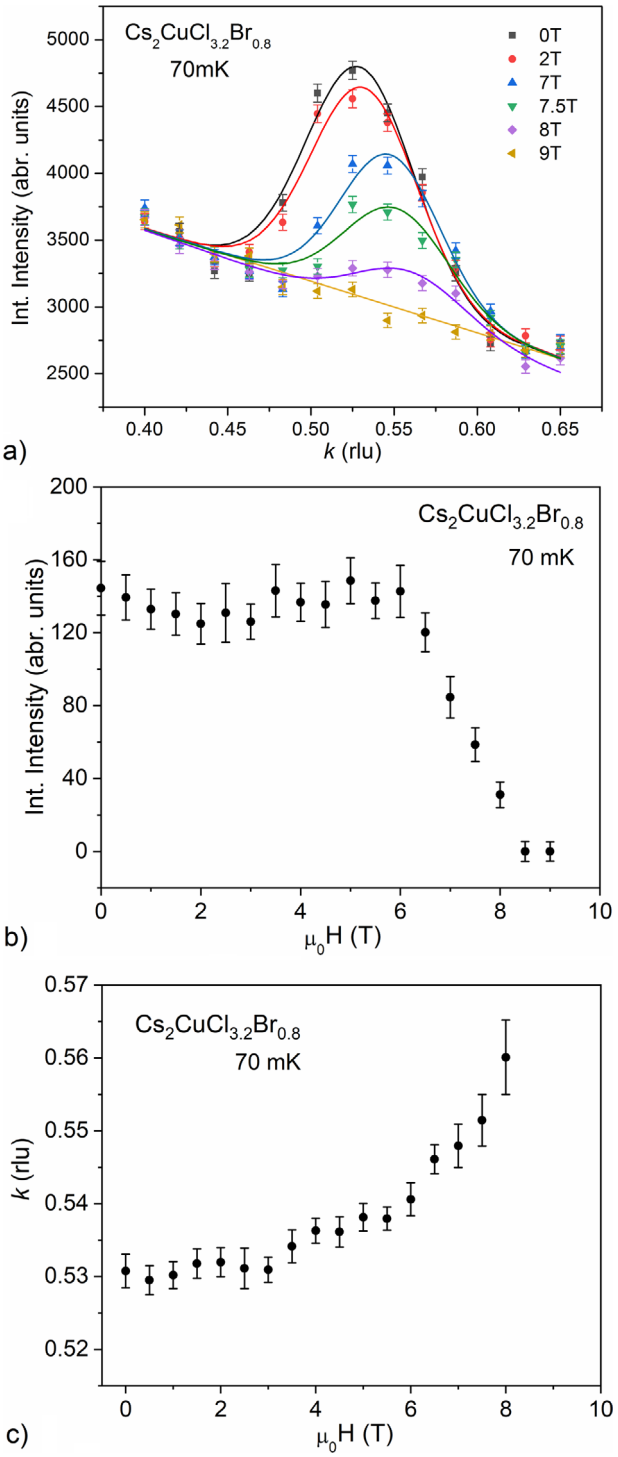

Figure 3. a) The intensity of the magnetic reflections for (0 *k* 0) of $Cs_2CuCl_{3.2}Br_{0.8}$ in a magnetic field (selected values) at 70 mK (Gaussian fits). b) Temperature dependence of the intensity of $Cs_2CuCl_{3.2}Br_{0.8}$ in a magnetic field up to 11.5 T at 70 mK. c) *k*-Values of $Cs_2CuCl_{3.2}Br_{0.8}$ as a function of the magnetic field at 70 mK.

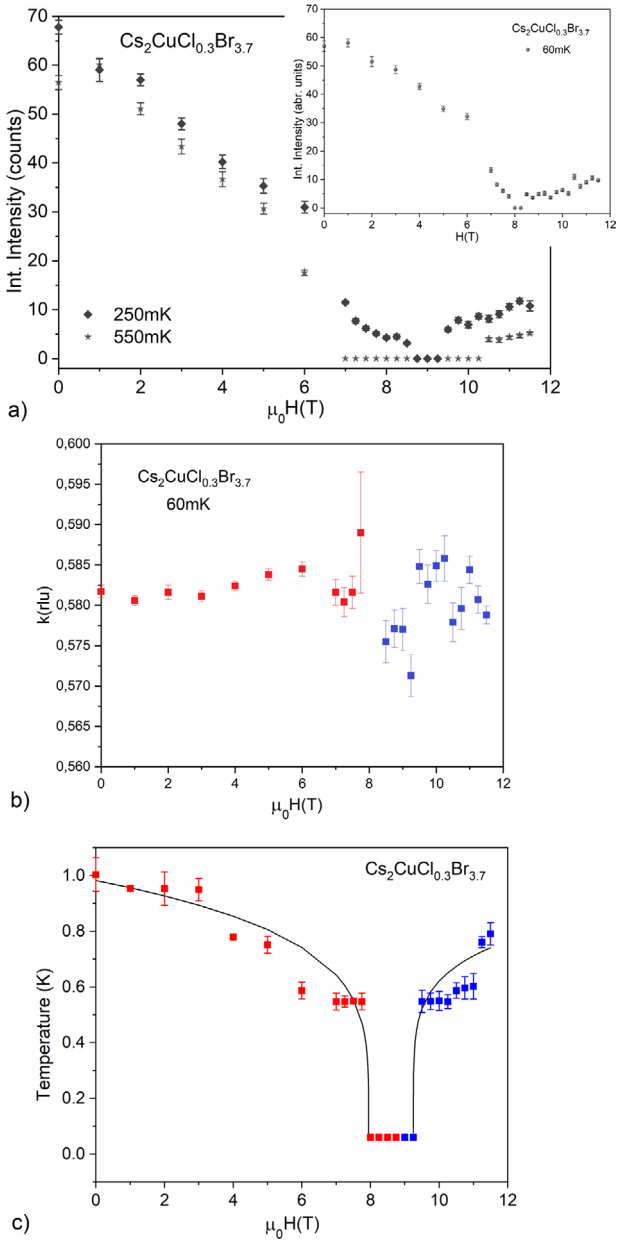

Figure 4. a) Temperature dependence of the intensity of $Cs_2CuCl_{0.3}Br_{3.7}$ in a magnetic field up to 11.5 T at 60, 250, and 550 mK. b) *k*-Values of $Cs_2CuCl_{0.3}Br_{3.7}$ depending on the magnetic field. c) Diagram of the critical magnetic field depending on the temperature (solid line: fit of power-law behavior for both magnetic phases).

The magnetic reflection exists up to the critical magnetic field of $B_c = 7.94(16)$ T for the first phase. At values of 8 and 8.25 T, no intensity of magnetic reflections is detected. However, intensities reappear for the next magnetic field value of 8.5 T and increase slightly till 11.5 T. This we interpret as evidence of two phases, below 7.94(16) T and above 8.5 T. Figure 4a shows the results for the measurements at 250 and 550 mK, which indicate that the separation region increases between the two magnetic phases.

The value of $k = 0.582(1)$ for $x = 3.7$ changes slightly with the temperature (see Figure 4b). This value is stable up to 8 T for the first magnetic phase. *k* changes from 0.582(8) in zero field to 0.589(7) at 7.75 T. This *k* value for the second magnetic phase is 0.578(7) and almost stable between 9 and 11.5 T. The changes of the position of the magnetic peak as a function of magnetic field is similar to that of Cs_2CuBr_4 measured parallel to the *a*-axis.[6] The ordering vector $q = (0, 0.575, 0)$ of Cs_2CuBr_4 shows a small anomaly in field dependence, when the field is parallel to the *a*-axis.[6] The value of *q* remains constant at low magnetic fields and exhibits a bend anomaly at a critical field around 7.5 T.[6] In both cases, the ordering wave vector in the magnetic field changes, which causes a change in the ratio J'/J.[17] For the new composition with $x = 3.7$, it can be seen experimentally that the low-field phase and the high-field phases are separated. Thus, the determination/calculation of the spin Hamiltonian parameters for these compositions cannot be performed simply above the Bc, because the change in the interaction reacts to the external magnetic field.

The diagram of the critical magnetic field depending on the temperature for $Cs_2CuCl_{0.3}Br_{3.7}$ is presented in Figure 4c, which shows a difference to that of Cs_2CuBr_4.[6] For that composition, Ono et al. find the phase transition to be around 7.5 T, which was detected with specific heat for a magnetic field parallel to the *a*-axis at $T = 0.6$ K and was also confirmed through a neutron scattering experiment.[6,14] Nevertheless, the separation of the two phases was not observed. The differences between $Cs_2CuCl_{0.3}Br_{3.7}$ and Cs_2CuBr_4 are caused by Cl doping.

Our investigations show that for Cs_2CuCl_4 and the investigated compositions of the mixed system, the magnetic vector *q* can be calculated as (0, 1-*k*, 0). Therefore, we conclude that the calculation of the respective magnetic vector should be the same for Cs_2CuBr_4. The experiments have shown that the magnetic structures in regimes I and IV are very different and have changed in magnetic field. The results of all investigations in magnetic field are summarized in **Figure 5**.

In the context of the investigations presented in this article, magnetic reflections were recorded only in the *bc*-plane. For a complete magnetic structure solution, other magnetic reflections of the *ab*-plane have to be included. For further investigations/calculations, it is necessary to understand, which magnetic structures occur depending on the magnetic field. Both the knowledge of the magnetic structure and the magnetic excitation dispersion need to be used for calculations of the exchange coupling parameters.

Coldea et al. constitute a two-spinon continuum in the spin liquid phase above T_N for Cs_2CuCl_4 and that the spin liquid phase is a 2D spin liquid (2D SL).[10,18] It still has to be confirmed with inelastic neutron scattering, whether the same applies for the part of the Br concentration range in regimes I and IV of this mixed system. Therefore, we have marked 2D SL in Figure 5 with "?." Regime III ($2 < x < 3.2$) shows no magnetic order in the magnetic phase diagram of $Cs_2CuCl_{4-x}Br_x$ for the compositions with $x = 2.2$ and 3.0.[15] We assume that this is a spin liquid phase. For compound $Cs_2CuCl_{1.8}Br_{2.2}$, the inelastic neutron scattering measurements were performed along (0 *k* 0) at 50 mK. **Figure 6** exhibits raw energy scans (without subtraction of the background) for the investigated direction.

The inset in Figure 6 shows the upper boundary of the continuum scattering at 1.5 meV, whereas for Cs_2CuCl_4, the upper boundary of the continuum scattering is at 1 meV.[10,18]

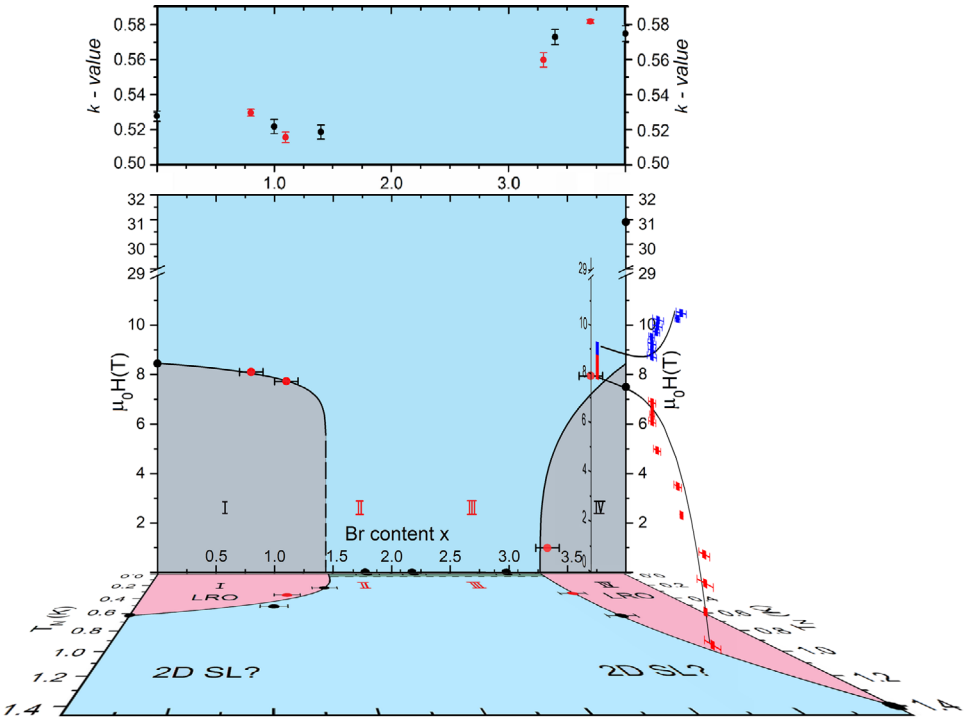

Figure 5. Magnetic phase diagram of $Cs_2CuCl_{4-x}Br_x$ in a magnetic field. The positions of the strongest magnetic reflections (k-value) are at the top (black and red circles) in regimes I and IV. At lower temperatures, a long-range magnetic order is observed for some compositions (black circles) in regimes I and IV (area in rose). The black circles show the data from literature;[5,6,15] the gray areas show the behavior in magnetic field up to 8.5 T. The red circles are the measured compositions with $x = 0.8$, 1.1, 3.3, 3.7; and a separation of two magnetic phases occurs in magnetic field for $Cs_2CuCl_{0.3}Br_{3.7}$. Magnetic properties below 0.05 K are not yet determined. The horizontal error bars ±0.1 represent the uncertainties in the EDX results of the chemical composition.

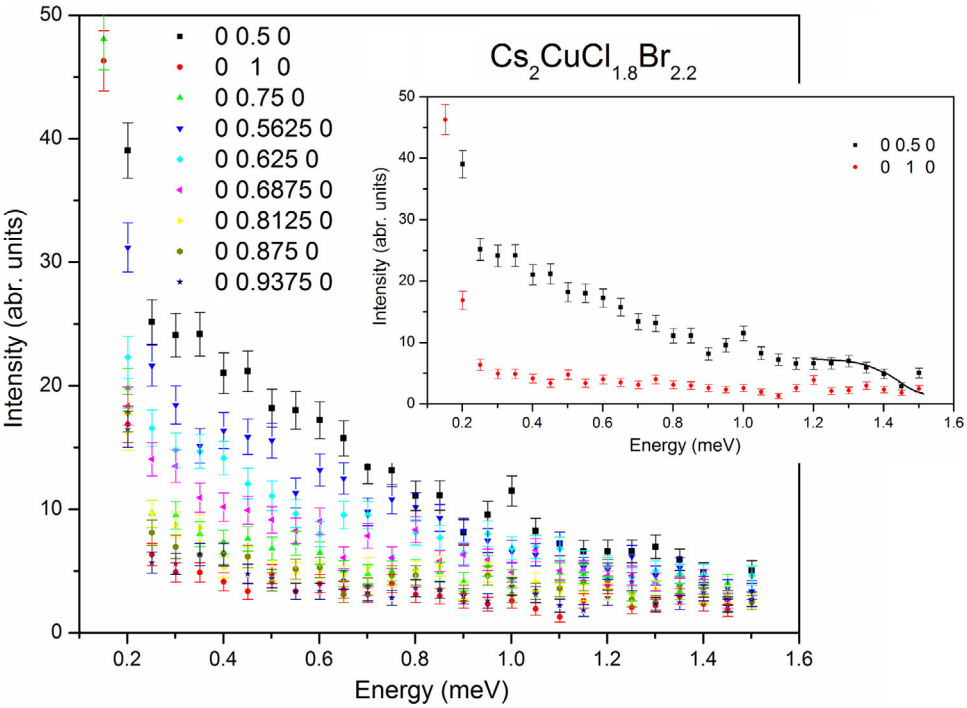

Figure 6. Energy scans along the (0 k 0) direction for $Cs_2CuCl_{1.8}Br_{2.2}$; the inset shows only two energy scans with a typical upper boundary of the continuum scattering (solid line as a guide to the eye).

This value is the same for the measurements above and below T_N.[18] This result at 1.5 meV suggests that the Br concentration in $Cs_2CuCl_{1.8}Br_{2.2}$ changes the upper boundary of the continuum scattering. For the intermediate concentration range ($1.5 < x < 3.2$), we assume two regimes, which show different mechanisms for the exchange coupling, depending on the Br concentration.[15] The discussion of the model for the interaction of regimes II and III in this mixed system is outlined in detail by van Well et al.[15] In general, the behavior of the exchange parameters was calculated from density functional theory calculations.

In literature, the spin liquid behavior is attributed to quasi-1D and less often to a 2D behavior with a two-spinon continuum. This topic is well-discussed in such systems.[4,19] The experimental data from this work and the data obtained by the inelastic neutron scattering experiment on Cs_2CuCl_4[10,18] show the same characteristic features, which are not yet fully described by the quasi 1D approach.[4] Further investigations of this spin liquid phase may clarify the dynamical correlations, which are dominated by highly dispersive scattering continua. They could be the hallmark of deconfined $S = 1/2$ spinons of a fractionalized phase. An important question is the nature of the fractionalized phase that dominates the physics in the $Cs_2CuCl_{4-x}Br_x$ mixed system. For example, for Cs_2CuCl_4, the description leads to strong two-spinon continua in the dynamical correlations.[18] There are various approaches, which are actively pursued in theory. The different compositions of the $Cs_2CuCl_{4-x}Br_x$ mixed system allow to study the nature of the fractionalized phase, depending on the Br concentration and the temperature, for example, above and below T_N for the area with LRO.

3. Experimental Section

Chemical Details for Crystal Growth: The $Cs_2CuCl_{4-x}Br_x$ crystals with an orthorhombic structure (*Pnma*) were grown with the evaporation method from aqueous solutions for the selected compositions. Single crystals were grown for nominal compositions with $x = 0.8$, 1.1, 2.2, 3.3, and 3.7. Stoichiometric mixtures of the salts CsCl/CsBr and $CuCl_2/CuBr_2$ were used for crystal growth.[14] Crystals generally grew within 6–8 months at a temperature of 323 K for $x = 2.2$ and 3.3, and at a temperature of 297 K for $x = 0.8$, 1.1, and 3.7.[20] For crystal growth, a constant temperature profile was used.

The chemical compositions of the samples were determined via energy dispersive X-ray analysis (EDX), using the electron microscope Zeiss Leo 1530. To facilitate the presentation, nominal values have been used throughout the study. The chemical composition of the samples has shown the following results in at%: Cs, 27.46 ± 0.21; Cu, 13.14 ± 0.23; Br, 55.84 ± 0.14; Cl, 3.56 ± 0.08. This outcome is consistent with the chemical formula of $Cs_2CuCl_{0.24}Br_{3.76}$.

Neutron Scattering

The crystals were oriented on ORION at SINQ of Paul Scherrer Institute (PSI) and on OrientExpress at Institut Laue-Langevin (ILL) in the *bc*-plane. The composition with $x = 2.2$ was orientated also in the *bc*-plane on neutron-Laue diffractometer RESI at FRM II of Heinz Maier-Leibnitz Zentrum (MLZ). Single-crystal neutron diffraction experiments were carried out on the thermal-neutron diffractometers ZEBRA at SINQ of PSI in Villigen, Switzerland and on the thermal-neutron two-axis diffractometer D23 at ILL in Grenoble, France.[21–24] A monochromatic neutron beam with wavelength 2.317 Å on ZEBRA was selected by a PG_{002}-monochromator and a PG_{002} filter. For $x = 1.1$ and $x = 3.3$, the nuclear structure was examined using single crystal neutron diffraction with $\lambda = 2.317$ Å at ZEBRA and corresponds to the above described orthorhombic structure (*Pnma*). The wavelengths 1.2732 and 2.3666 Å were used on D23 with Cu_{200} and PG_{002} monochromators. For detection of magnetic reflections, the wavelengths 2.3666 Å and an analyzer were utilized. At D23, the nuclear structure was proved using neutron diffraction with a wavelength $\lambda = 1.2732$ Å. The refinement for the collected data with an orthorhombic structure (*Pnma*) resulted in $R_F = 6.6\%$ and $R_F = 5.2\%$, respectively, for $x = 0.8$ and $x = 3.7$. On both diffractometers, normal beam geometry was applied. The diffracted signal was collected with a single ^{3}He–tube detector.

Single-crystal neutron diffraction was also performed on the cold-three-axes spectrometer MIRA at FRM II of MLZ in Garching, Germany.[25] For the elastic measurements, a wavelength of 4.488 Å ($k_i = 1.4$ Å^{-1}) was applied by means of a PG_{002} monochromator. For the inelastic neutron scattering measurements, a final wave vector $k_f = 1.550$ Å^{-1} came into operation. A Be-filter and a single ^{3}He-tube detector were utilized. The crystals were cooled down to 50 mK with a dilution cryostat.

Acknowledgements

The authors thank Ch. Rüegg from the Department for Research with Neutrons and Muons (PSI), Villigen, Switzerland for fruitful discussions. The authors thank M. Heider from Bayerisches Polymerinstitut, Bayreuth, Germany for her support. The neutron diffraction experiments were performed on ZEBRA with crystals orientated on ORION at PSI, Villigen, Switzerland and on D23 with crystals orientated on OrientExpress at ILL, Grenoble, France. The authors also thank B. Pedersen for the orientation of the crystals on the neutron-laue diffractometer RESI at FRM II of MLZ, Garching, Germany. The neutron scattering experiments were performed on MIRA at FRM II of MLZ, Garching, Germany. This work was supported by Paul Scherrer Institute, Institut Laue-Langevin, University of Bayreuth, Heinz Maier-Leibnitz Zentrum and Physik Department E21, Technische Universität München, and the Deutsche Forschungsgemeinschaft through the research fellowship for the project WE-5803/1-1 and WE-5803/2-1, and through the fellowship A 4576—1/3 of the University of Bayreuth. This work was additionally supported by the Swiss State Secretariat for Education, Research and Innovation (SERI) through a CRG-grant.

Conflict of Interest

The authors declare no conflict of interest.

Keywords

$Cs_2CuCl_{4-x}Br_x$ mixed system, magnetic order

Received: March 20, 2020
Revised: April 28, 2020
Published online: June 9, 2020

[1] M. Vojta, *Rep. Prog. Phys.* **2018**, *81*, 064501.
[2] S. A. Zvyagin, D. Graf, T. Sakurai, S. Kimura, H. Nojiri, J. Wosnitza, H. Ohta, T. Ono, H. Tanaka, *Nat. Commun.* **2019**, *10*, 1064.
[3] S. Sachdev, B. Keimer, *Phys. Today* **2011**, *64*, 29.
[4] M. Kohno, O. A. Starykh, L. Balents, *Nat. Phys.* **2007**, *3*, 790.
[5] R. Coldea, D. A. Tennant, R. A. Cowley, D. F. McMorrow, B. Dorner, Z. Tylczynski, *J. Phys.: Condens. Matter* **1996**, *8*, 7473.

[6] T. Ono, H. Tanaka, T. Nakagomi, O. Kolomiyets, H. Mitamura, F. Ishikawa, T. Goto, K. Nakajima, A. Oosawa, Y. Koike, K. Kakurai, J. Klenke, P. Smeibidle, M. Meißner, H. A. Katori, *J. Phys. Soc. Jpn.* **2005**, *74*, 135.
[7] S. A. Zvyagin, D. Kamenskyi, M. Ozerov, J. Wosnitza, M. Ikeda, T. Fujita, M. Hagiwara, A. I. Smirnov, T. A. Soldatov, A. Ya. Shapiro, J. Krzystek, R. Hu, H. Ryu, C. Petrovic, M. E. Zhitomirsky, *Phys. Rev. Lett.* **2014**, *112*, 077206.
[8] R. Coldea, D. A. Tennant, K. Habicht, P. Smeibidl, C. Wolters, Z. Tylczynski, *Phys. Rev. Lett.* **2002**, *88*, 137203.
[9] R. Coldea, D. A. Tennant, A. M. Tsvelik, Z. Tylczynski, *Phys. Rev. Lett.* **2001**, *86*, 1335.
[10] R. Coldea, D. A. Tennant, Z. Tylczynski, *Phys. Rev. B* **2003**, *68*, 134424.
[11] T. Radu, H. Wilhelm, V. Yushankhai, D. Kovrizhin, R. Coldea, Z. Tylczynski, T. Lühmann, F. Steglich, *Phys. Rev. Lett.* **2005**, *95*, 127202.
[12] T. Ono, H. Tanaka, H. Aruga Katori, F. Ishikawa, H. Mitamura, T. Goto, *Phys. Rev. B* **2003**, *67*, 104431.
[13] Y. Tokiwa, T. Radu, R. Coldea, H. Wilhelm, Z. Tylczynski, F. Steglich, *Phys. Rev. B* **2006**, *73*, 134414.
[14] N. Kruger, S. Belz, F. Schossau, A. A. Haghighirad, P. T. Cong, B. Wolf, S. Gottlieb-Schoenmeyer, F. Ritter, W. Assmus, *Cryst. Growth Des.* **2010**, *10*, 4456.
[15] N. van Well, O. Zaharko, B. Delley, M. Skoulatos, R. Georgii, S. van Smaalen, C. Rüegg, *Ann. Phys.* **2018**, *530*, 1800270.
[16] N. van Well, K. Foyevtsova, S. Gottlieb-Schoenmeyer, F. Ritter, B. Wolf, M. Meven, C. Pfleiderer, M. Lang, W. Assmus, R. Valenti, C. Krellner, *Phys. Rev. B* **2015**, *91*, 035124.
[17] J. O. Fjærestad, W. Zheng, R. R. P. Singh, R. H. McKenzie, R. Coldea, *Phys. Rev. B* **2007**, *75*, 174447.
[18] R. Coldea, D. A. Tennant, Z. Tylczynski, *J. Magn. Magn. Mater.* **2004**, *272–276*, E649.
[19] O. A. Starykh, H. Katsura, L. Balents, *Phys. Rev. B* **2010**, *82*, 014421.
[20] N. van Well, *Innovative und interdisziplinare Kristallzüchtung*, Springer Spektrum, Wiesbaden, Germany **2016**.
[21] J. Schefer, P. Fischer, H. Heer, A. Isacson, M. Koch, R. Thut, *Nucl. Instrum. Methods Phys. Res., Sect. A* **1990**, *288*, 477.
[22] J. Schefer, M. Könnecke, A. Murasik, A. Czopnik, T. Strässle, P. Keller, N. Schlumpf, *Phys. B* **2000**, *276–278*, 168.
[23] Paul Scherrer Institut homepage, https://www.psi.ch/sinq/zebra/description (accessed: May 2020).
[24] Institut Laue-Langevin homepage, https://www.ill.ev/users/instruments-list/d23 (accessed: May 2020).
[25] R. Georgii, T. Weber, G. Brandl, M. Skoulatos, M. Janoschek, S. Muhlbauer, C. Pfleiderer, P. Böni, *Nucl. Instrum. Methods Phys. Res., Sect. A* **2018**, *881*, 60.